Available online at www.sciencedirect.com

ScienceDirect

Ceramics International 40 (2014) 2585–2592

CERAMICS INTERNATIONAL

www.elsevier.com/locate/ceramint

Effects of CuO addition on the structure and electrical properties of low temperature sintered $Ba(Zr,Ti)O_3$ lead-free piezoelectric ceramics

Dayun Liang, Xiaohong Zhu*, Jiliang Zhu, Jianguo Zhu, Dingquan Xiao

Department of Materials Science, Sichuan University, Chengdu 610064, PR China

Received 14 October 2013; received in revised form 16 October 2013; accepted 16 October 2013
Available online 25 October 2013

Abstract

CuO-doped $Ba(Zr_{0.05}Ti_{0.95})O_3$ (BZT) ceramics were prepared using conventional solid state reaction method, and their structure and electrical properties were investigated. It was found that a small amount of CuO could lower the sintering temperature significantly and make their microstructure more densified than pure BZT. The ceramics with 1.2 mol% CuO, sintered at 1250 °C, showed excellent piezoelectric properties with $d_{33}\sim 320$ pC/N and $k_p=44\%$. The sintering temperature was decreased by 150 °C than that for pure BZT ceramics while showing comparable piezoelectric properties. Moreover, the influence of sintering temperature on the optimally 1.2 mol% CuO-doped BZT ceramics was studied. With the temperature change, different patterns of crystal growth were observed in the doped BZT ceramics. When the sintering temperature increased from 1200 °C to 1350 °C, the patterns of normal–abnormal–normal grain growth were changed accordingly.

Keywords: Electrical properties; $Ba(Zr,Ti)O_3$; Lead-free piezoelectric ceramics; Structure; Sintering temperature

1. Introduction

In recent years, $BaTiO_3$-based ceramics have received much attention from the scientific community in the process of searching for the lead-free ferroelectric materials [1–12]. Through chemical substitutions for A sites or B sites in $BaTiO_3$ ceramics, the different electrical properties can be acquired to meet our requirements for specific utilization. Among them, $Ba(Zr_xTi_{1-x})O_3$ (BZT) solid solution has attracted considerable attention for its special characteristics. Through modifying the Ti^{4+}/Zr^{4+} ratio of the BZT material, its three phase transition temperatures of rhombohedral–orthorhombic (T_{R-O}), orthorhombic–tetragonal (T_{O-T}) and tetragonal–cubic (T_C) phase transitions can be shifted[4–8], and then desired piezoelectricity, dielectric relaxation and tunability can be developed with specific zirconium content, resulting in wide use for various device applications, such as piezoelectric transducers, dynamic random access memories, tunable microwave devices, and so on [9–12].

However, the homogeneous and dense microstructure is quite hard to be obtained in BZT ceramics, and their sintering temperatures are usually required to be as high as 1400–1500 °C. These drawbacks severely restrict their practical applications [4–8,13–15]. Recently, much effort has been taken to find sintering aids, such as CuO, Li_2O, MnO_2, Bi_2O_3 [16–20]. CuO, as an additive, may result in liquid phase sintering in ceramics, thereby significantly promoting the densification, lowering the sintering temperature, and improving the electrical properties of ceramics. Hence, it was widely used in lead-free piezoelectric $(Bi,Na)TiO_3$ and $(K,Na)NbO_3$ systems [21–25]. Nonetheless, its effect on the microstructure and piezoelectric properties of BZT ceramics as a sintering aid has been seldom reported.

In this work, we investigate systematically the microstructure and electrical properties of CuO-modified BZT ceramics. $Ba(Zr_{0.05}Ti_{0.95})O_3$ has excellent piezoelectric performance (as shown in Fig. 1) and relatively high Curie temperature, it was therefore chosen as the matrix material.

2. Experimental procedure

BZT + x mol% CuO ceramics with $x=0$, 0.2, 0.7, 1.2 and 4.0 were fabricated by the solid state reaction route. The raw materials were $BaCO_3$ (99%), TiO_2 (98%) and ZrO_2 (99%).

*Corresponding author. Tel.: +86 28 85412415; fax: +86 28 85416050.
E-mail address: xhzhu@scu.edu.cn (X. Zhu).

0272-8842/$ - see front matter © 2013 Elsevier Ltd and Techna Group S.r.l. All rights reserved.
http://dx.doi.org/10.1016/j.ceramint.2013.10.084

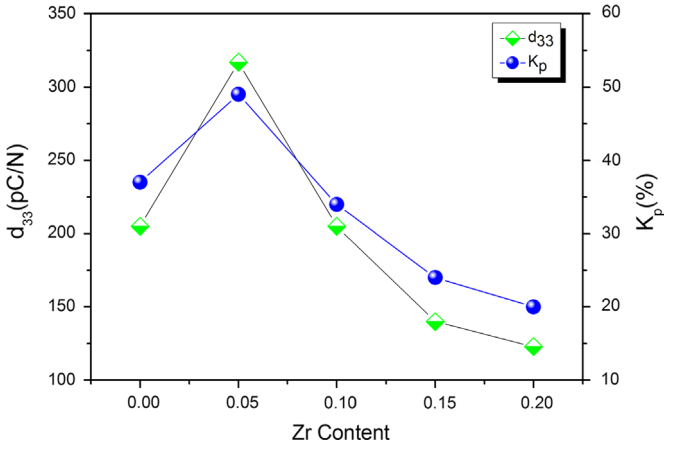

Fig. 1. The piezoelectric coefficient d_{33} and planar mode electromechanical coupling coefficient k_p of the BZT ceramics as a function of the zirconium content. All the samples were sintered at 1400 °C.

The raw powder was thoroughly ball mixed with ZrO_2 balls for 24 h using ethanol as the medium. The homogeneous mixtures were calcined at 1250 °C, and then the pre-synthesized BZT powder and CuO powder were mixed according to the formula and re-milled for 24 h. The powders were subsequently mixed with a polyvinyl alcohol (PVA) binder solution and compacted into disk samples with a diameter of ~1.0 cm and a thickness of ~1.0 mm. After burning out PVA at 850 °C for 2 h, pellets of CuO-doped BZT were sintered at 1200–1350 °C for 3 h, while the pure BZT was sintered at 1400 °C. Then the silver pastes were fired at 800 °C for both sides of these samples as electrodes for electrical measurements. All samples were poled at room temperature of 25 °C in a silicone oil bath under a DC field of 3.0 kV/mm for 10 min.

The phase structure of these ceramics was measured using X-ray diffraction (XRD) (DX1000, PR China). Surface morphologies of the specimens were determined by scanning electron microscopy (SEM) (Philips, XL30). The dielectric properties of these ceramics were firstly evaluated using a TH2816 LCR meter at 1 kHz, and then the dielectric behavior as a function of the measurement temperature was carefully measured by using a programmable furnace with an LCR analyzer (HP 4980, Agilent, USA). The piezoelectric constant d_{33} of the ceramics was measured using a piezo-d_{33} meter (ZJ-3A, China). The polarization versus electric field (P–E) hysteresis loops of the ceramics were measured using a Radiant Precision Workstation (Radiant Technologies, Inc., USA) at 20 Hz.

3. Results and discussion

3.1. Effect of CuO content on the structural and electrical properties of the ceramics

The crystal structure of the BZT+x mol% CuO ceramics with x=0, 0.2, 0.7, 1.2 and 4.0 was determined by X-ray diffraction. As shown in Fig. 2, all the samples exhibited pure orthorhombic perovskite structure as $Ba(Zr_{0.05}Ti_{0.95})O_3$ and no second phase was detected within the resolution limit of the apparatus [12,26,27]. However, the lattice parameter was affected by the introduction of CuO addition. The refined XRD patterns reveal that the XRD peak of the CuO-modified BZT ceramics was shifted to lower angle with increase of CuO content, indicating an increase of lattice parameter in the specimens. Considering that the ionic radius of Cu^{2+} (0.73 Å) is larger than both Zr^{4+} (0.72 Å) and Ti^{4+} (0.605 Å), it is hard to enter the interstitial positions of crystals, so we can reasonably speculate that some Cu^{2+} ions enter the B-site of the BZT ceramics, leading to an increase of lattice parameter [23,28]. However, when $x>1.2$, owing to the limit of solid solubility of Cu^{2+} ions in the BZT matrix, the excessive Cu^{2+} ions concentrate on the grain boundary, thereby the crystal lattice does not increase any more with further increase of CuO content, as shown in Fig. 2(b).

The surface morphologies of the BZT ceramics with different CuO contents are shown in Fig. 3. When x=0.2, the BZT ceramics show a porous surface morphology, and the grain size is fairly small, indicating the process of grain growth was incomplete. As the CuO content increases, the microstructure of the ceramics becomes denser and the grain size increases monotonously. Specifically, when x increases to 4.0, the extremely coarse grain was observed, as shown in Fig. 3(d). This is similar to what was observed in the pure BZT ceramics sintered at 1400 °C, as presented in the inset of Fig. 3(d). Besides, some thin amorphous intergranular phase appeared at grain boundaries and triple conjunctions [29]. This may be related to complex oxide of copper and other impurities. Just as the analysis in XRD profiles, due to the limit of solid solubility of Cu^{2+} ions in the BZT matrix, the excessive copper and other impurities should separate out and concentrate at the grain boundaries and triple conjunctions, as shown in Fig. 3(d). In contrast to the pure BZT ceramics, the CuO modified samples have denser microstructure; meanwhile, their grain morphologies are more homogeneous. The microstructural improvement in the CuO-modified BZT ceramics may be caused by the liquid phase sintering effect due to the introduction of CuO sintering aid [22,23,25]. Because the grains were enclosed by liquid phase in the sintering process, the grain growth tended to be isotropic, and thus the spherical grains were developed finally.

Fig. 4 plots the temperature dependence of the dielectric properties for the BZT ceramics doped with different CuO contents, namely, x=0.2, 0.7, 1.2 and 4.0 mol%. From Fig. 4 (a)–(d) we can see that a small amount of CuO additive has no obvious influence on the cubic–tetragonal phase transition (T_C). However, the ceramics with 0.2 and 0.7 mol% CuO additives display a diffuse phase transition (DPT) characteristic for both T_C and T_{O-T} transitions. With the increasing of CuO content, the T_C transition peak becomes sharper and the T_{O-T} transition peak becomes more obvious gradually, as shown in Fig. 4(c) and (d). Besides, we also notice that the BZT+4.0 mol% CuO ceramic has much higher dielectric losses than the ceramics with x=0.2, 0.7 and 1.2. This may be attributed to the excessively doped CuO additives, as shown in Fig. 3(d).

Fig. 5 plots the room temperature polarization–electric field (P–E) hysteresis loops for the BZT ceramics with different CuO contents. As shown in Fig. 5(a), the sample with 0.2 mol

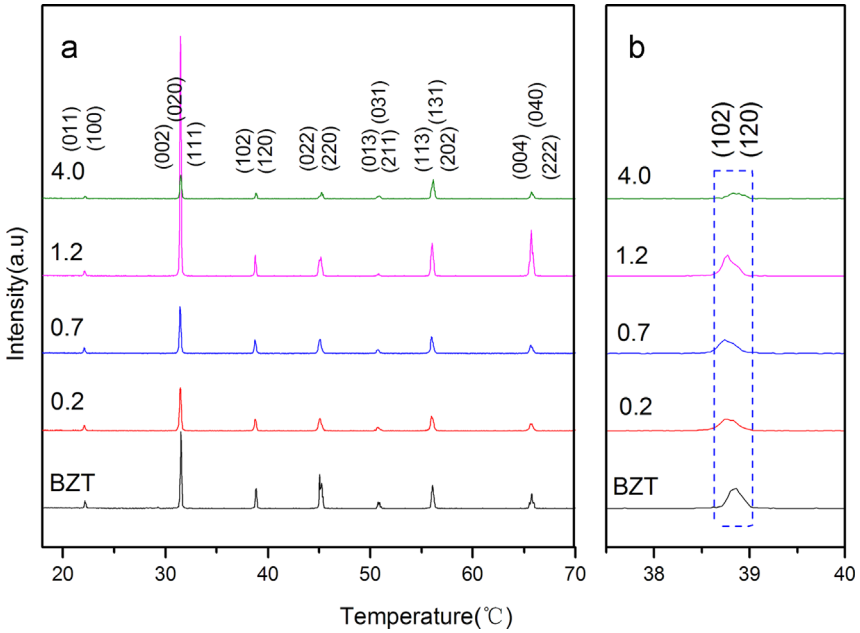

Fig. 2. X-ray diffraction patterns of the BZT+x mol% CuO ceramics with x=0, 0.2, 0.7, 1.2 and 4.0. The BZT ceramics with CuO additives were sintered at 1250 °C, while the pure BZT ceramics were sintered at 1400 °C.

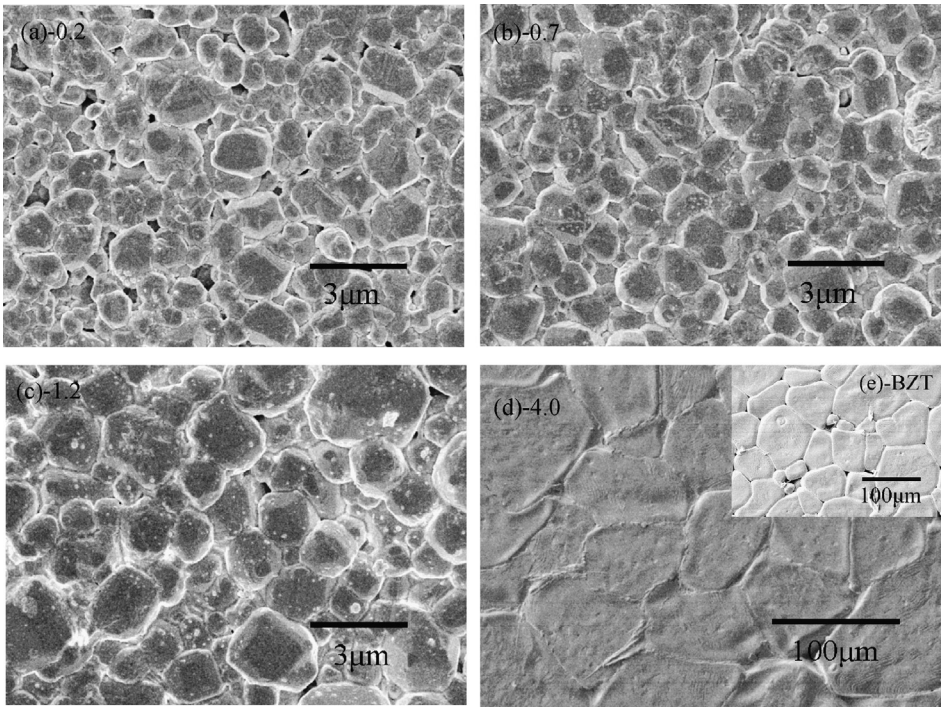

Fig. 3. Surface morphologies of the BZT ceramics with different CuO contents detected by SEM.

% CuO presents an unsaturated *P–E* loop. This is mainly caused by the high leakage current due to the porous microstructure, as shown in Fig. 2(a). Note that with the increase in CuO content, the ceramics begin to present the typical *P–E* loop characteristic with reduced loop area and sharpened saturated polarization, as shown in Fig. 5(b)–(d). We also notice that the BZT ceramic with 1.2 mol% CuO possesses the minimum coercive field with $E_c \sim 0.16$ kV/mm, which is even smaller than that for the 1400 °C-sintered BZT with no CuO addition. By contrast, the coercive field is increased again for the BZT ceramic with 4.0 mol% CuO, which becomes much larger than that for the BZT with 1.2 mol % CuO. This is probably because the ceramics become "hard" with excessively doped CuO, as discussed in the XRD profiles. Doping of CuO into the BZT ceramics leads to a small amount of Ti^{4+} substituted by Cu^{2+}, thereby a certain amount of

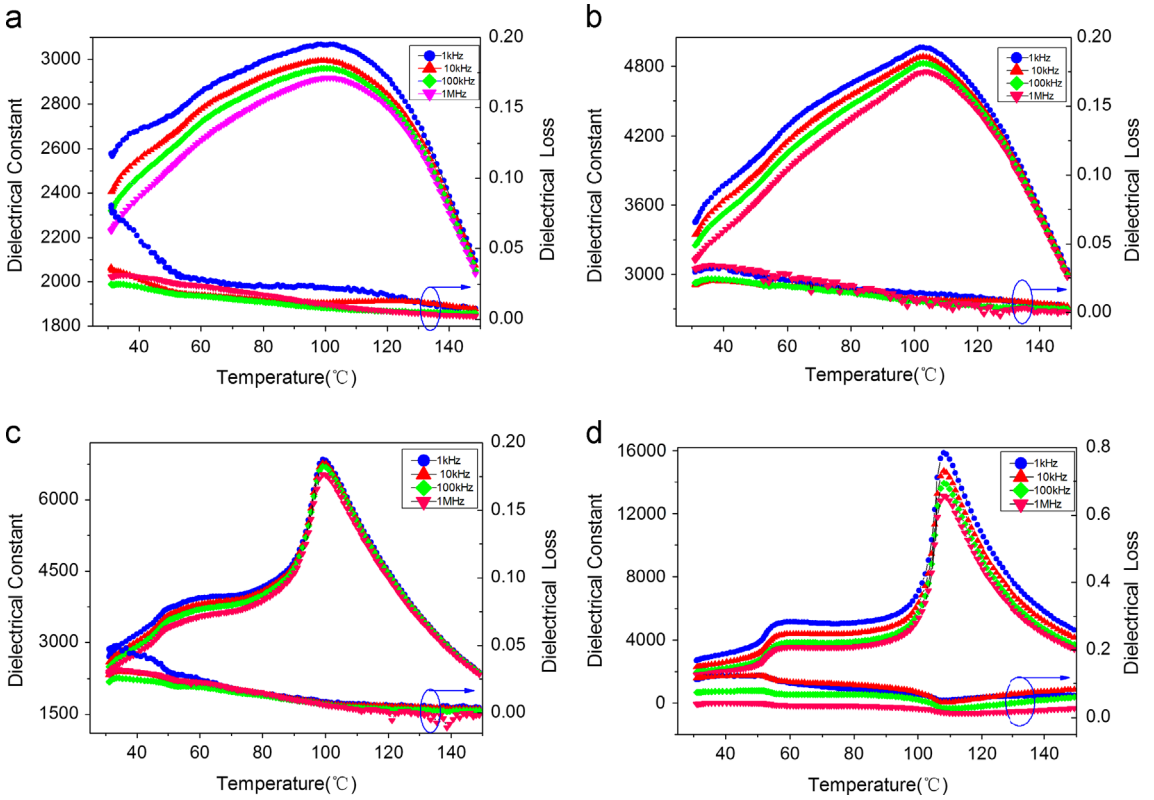

Fig. 4. Temperature dependence of the dielectric properties of the BZT ceramics doped with different CuO contents, i.e., x=0.2, 0.7, 1.2 and 4.0 mol%.

oxygen vacancies are generated with the presence of excess cupric ions in samples, i.e., the so-called defect dipoles are formed. The defect dipoles have a pinning effect on the ferroelectric domain switching, eventually increasing the coercive field [17,23,24].

Fig. 6 plots the piezoelectric coefficient d_{33} and planar mode electromechanical coupling coefficient k_p of the CuO modified BZT ceramics as a function of the CuO content. With a small amount of CuO additives mixed in the BZT matrix, the d_{33} and k_p values increase rapidly, then reach their maximum values with $d_{33}\sim$320 pC/N and $k_p\sim$44% at x=1.2. This d_{33} result is much better than those reported in the literature, where $d_{33}\sim$208 pC/N for the BZT ceramics sintered at 1400 °C [6] and $d_{33}\sim$266 pC/N for the BZT ceramics sintered at 1450 °C [27]. The enhanced piezoelectric properties are mainly attributed to the densified microstructure and enlarged grain size of the ceramics, benefited from the liquid phase sintering due to the introduction of CuO sintering aids. Furthermore, the occurrence of orthorhombic–tetragonal phase transition near room temperature (Fig. 4) and the minimal E_c value of the BZT–1.2 mol% CuO ceramics (Fig. 5) are also favorable to the high piezoelectric performance. It should be pointed out that the d_{33} and k_p drop respectively to a lower value slightly when x=4.0. This could be explained as follows: the enhanced piezoelectric properties by enlarged grain size and densified microstructure are partially canceled out by the 'hardening' effect of CuO and the existence of the amorphous intergranular phase in ceramics, as analyzed above.

3.2. Effect of sintering temperature on $Ba(Zr_{0.05}Ti_{0.95})O_3$–1.2 mol% CuO (abbreviated as BZT–12Cu) ceramics

The XRD patterns of the BZT–12Cu ceramics sintered at different temperature are shown in Fig. 7. As can be seen, all the samples present similar orthorhombic perovskite phase structure [12,26,27]. However, as the sintering temperature increases to 1300 °C, a second phase, revealed by the diffraction peak at 2θ=28.7°, begins to appear, then becomes distinct with further increase in temperature, indicating that too high sintering temperature may result in the appearance of second phase.

The surface morphologies of the BZT–12Cu ceramics sintered at different temperatures are shown in Fig. 8. It is noteworthy that different microstructures and grain morphologies were observed for the ceramics sintered at different temperatures. As shown in Fig. 8(a), the ceramic even sintered at 1200 °C has dense microstructure with homogeneous and small spherical grains. However, when the sintering temperature was increased to 1250 °C, an interesting phenomenon was observed. With the appearance of abnormal grain growth (AGG), the distribution of grain size presents a typical bimodal characteristic. A small fraction of coarse grains are surrounded by a large amount of fine grains and grow up rapidly through consuming them. From the magnified image, as shown in the inset of Fig. 8(b), we can see that the coarse grains have faceted and straight grain boundary with hill-and-valley shapes, as similarly observed in alumina [29]. It is proposed

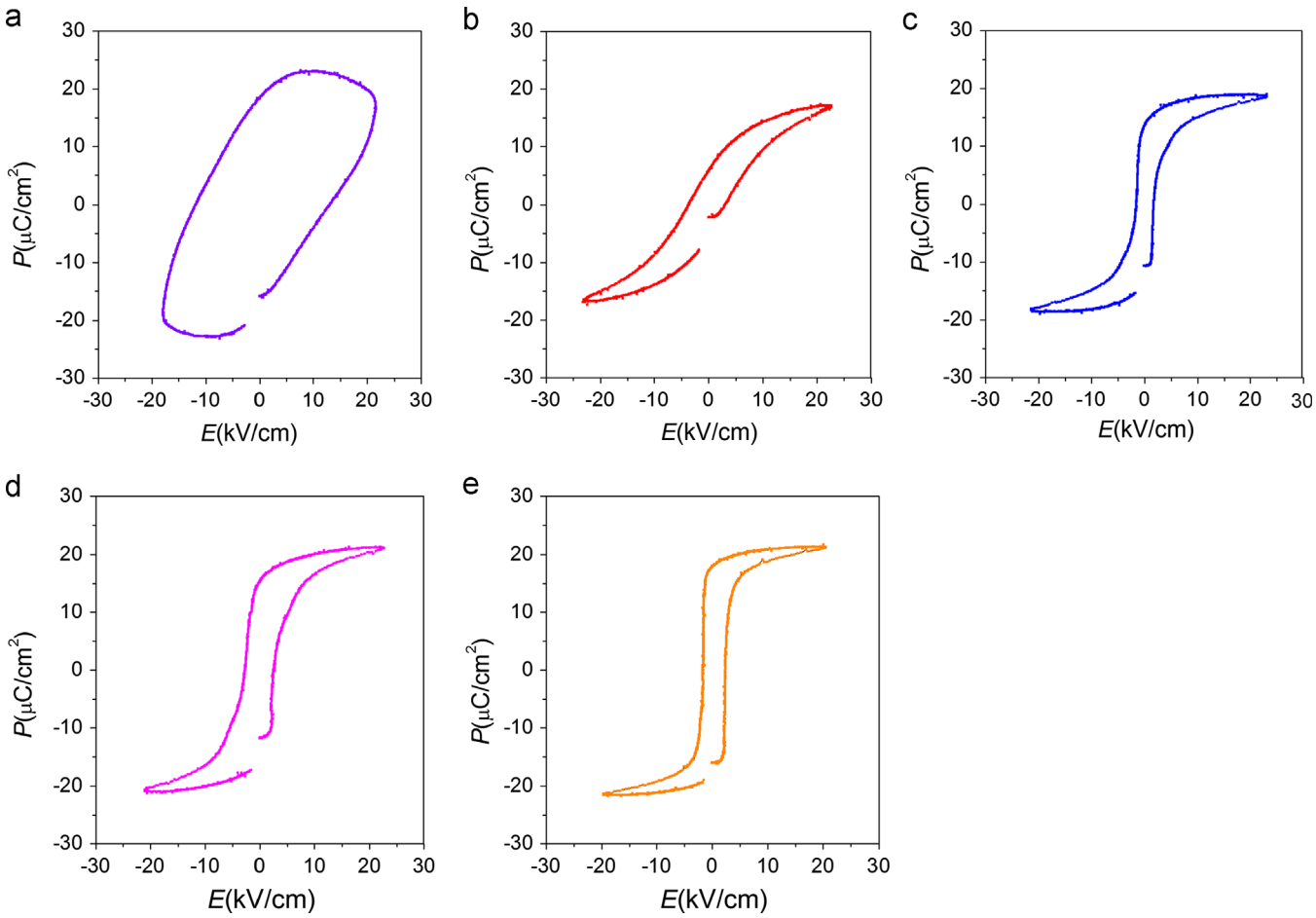

Fig. 5. Room temperature polarization–electric field (*P*–*E*) hysteresis loops for the BZT ceramics with different CuO contents of $x=0$, 0.2, 0.7, 1.2 and 4.0.

that these grain boundaries have singular ordered structures with low boundary energies and their growth by lateral step movement can cause the AGG [29,30]. The occurrence of AGG could be explained by a two-dimensional nucleation mechanism, as already discussed in Refs. [31,32]. As the sintering temperature further increases, however, the grain morphology changes again. Once fine matrix grains are completely replaced by coarse grains, the angular grains with flat surface and lath shape elongated at one particular direction appear. Further grain growth is retarded and the distribution of grain size starts a trend to be uniform at this stage, as shown in Fig. 8(c) and (d). Besides, the excessive sintering temperature leads to the occurrence of amorphous intergranular phase, as shown in Fig. 8(d), which was concentrated at the grain boundaries or triple conjunctions with the growth of grains. The observance of amorphous intergranular phase here is in good agreement with the second phase observed in XRD profile as shown in Fig. 7.

The temperature dependence of the dielectric properties of the BZT–12Cu ceramics sintered at different temperatures is shown in Fig. 9. The tetragonal–cubic phase transition at T_C was observed in all the samples. It is noted that the sintering temperature has no obvious influence on T_C of the ceramics, which is maintained at about 100–110 °C; however, the dielectric constant at T_C is increased and the phase transition peak becomes sharper with increasing the sintering temperature.

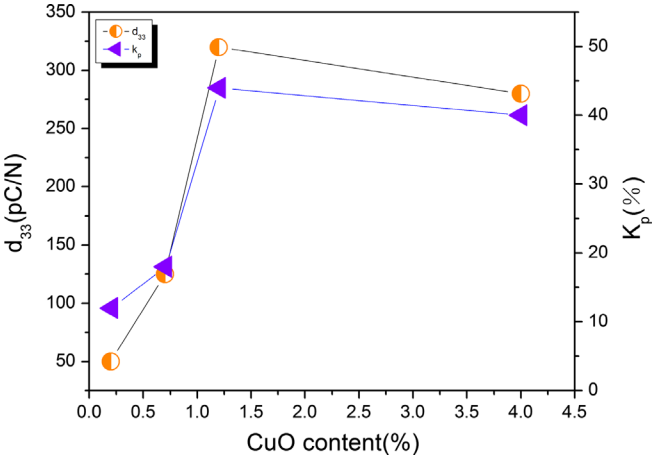

Fig. 6. The piezoelectric coefficient d_{33} and planar mode electromechanical coupling coefficient k_p of the CuO modified BZT ceramics as a function of the CuO content.

Fig. 10 plots the room temperature *P*–*E* hysteresis loops for the BZT–12Cu ceramics. It can be seen that all the ceramic samples exhibit saturated rectangle loops except the sample

sintered at 1200 °C. The remanent polarization increases slightly with the increase of sintering temperature, while the coercive field maintains low. The piezoelectric properties as a function of the sintering temperature are shown in Fig. 11. As can be seen, both the piezoelectric constant d_{33} and the planar mode electromechanical coupling coefficient k_p increase rapidly when the sintering temperature is below 1250 °C. However, the piezoelectric performance has no obvious enhancement when the sintering temperature further increases from 1250 °C to 1350 °C, although the grain size keeps on increasing. This may be attributed to the compromise between the enlarged grain size and the second phase arising from high sintering temperature. It is known that these two factors can enhance and lower the piezoelectric properties. In combination, the ceramics sintered at 1250 °C show preferable overall performance.

4. Conclusions

In this work, we have investigated the influence of CuO additive content and sintering temperature on the structure and electrical properties of BZT ceramics. It is demonstrated that a small amount of Cu^{2+} ions can enter the crystal lattice to substitute Ti^{4+} ions and change the lattice constant, but excess CuO additive may result in the occurrence of some thin amorphous intergranular phase at the grain boundaries and

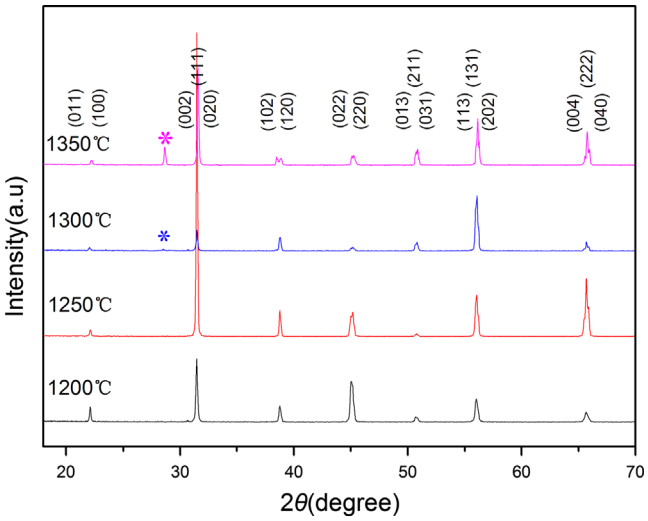

Fig. 7. X-ray diffraction patterns of the BZT–12Cu ceramics sintered at different temperatures.

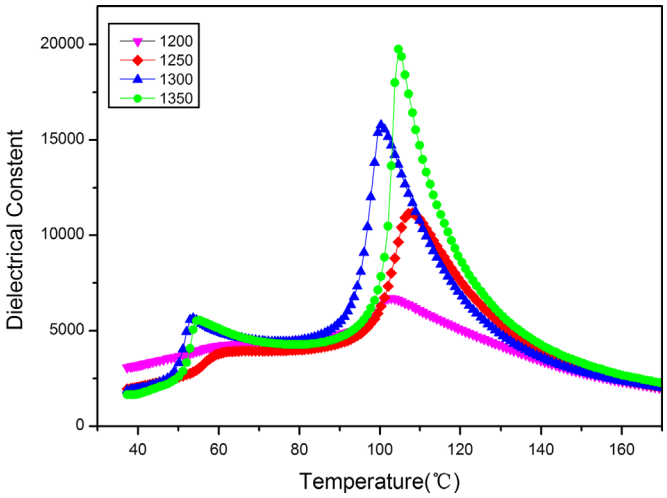

Fig. 9. Temperature dependence of the dielectric properties of the BZT–12Cu ceramics sintered at different temperatures.

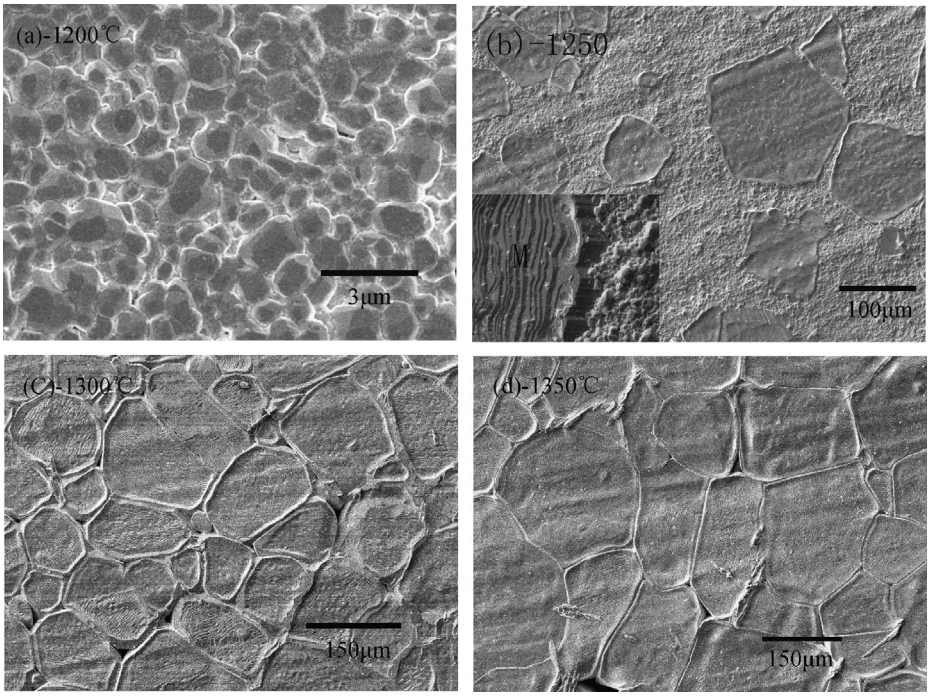

Fig. 8. Surface morphologies of the BZT–12Cu ceramics sintered at different temperatures detected by SEM.

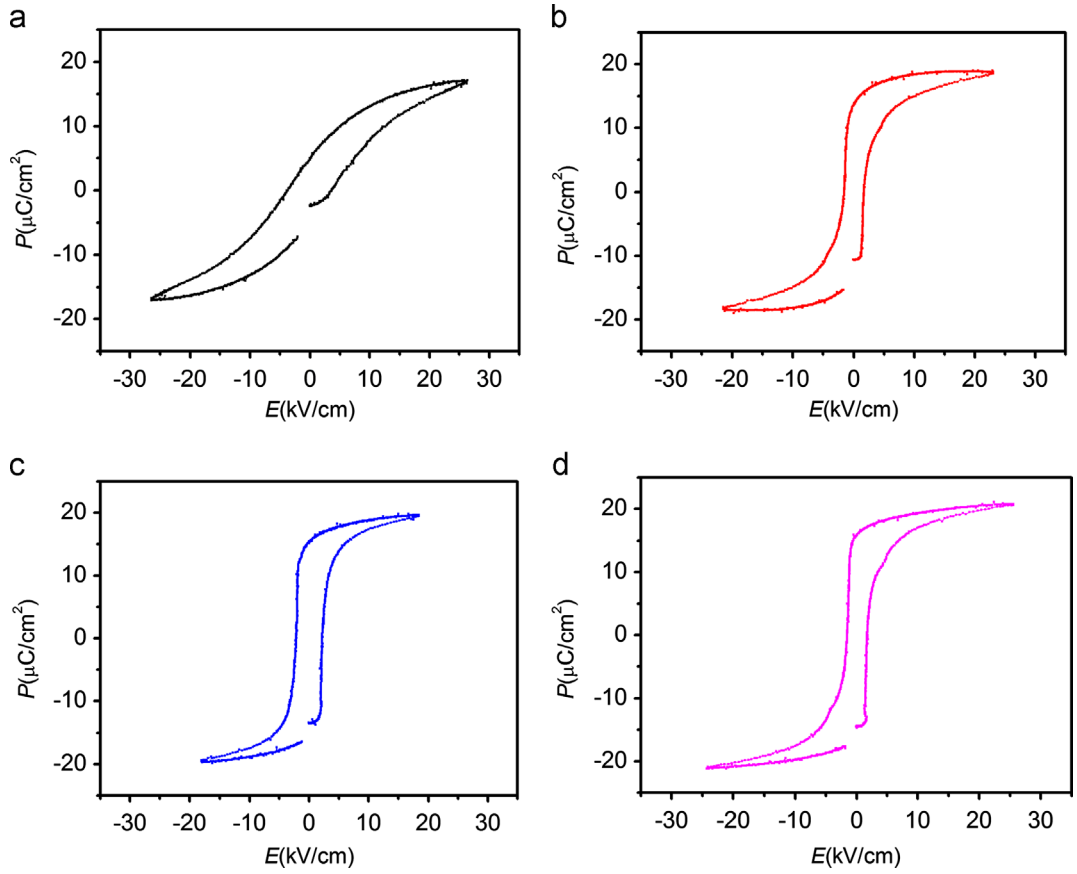

Fig. 10. Room temperature polarization–electric field (P–E) hysteresis loops for the BZT–12Cu ceramics sintered at different temperatures.

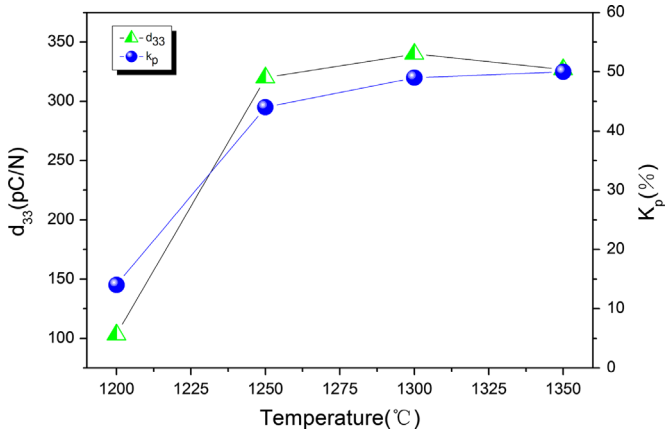

Fig. 11. The piezoelectric coefficient d_{33} and planar mode electromechanical coupling coefficient k_p of the BZT–12Cu ceramics as a function of the sintering temperature.

triple junctions, which has a negative effect on the piezoelectric performance of ceramics. The best piezoelectric properties with $d_{33}\sim320$ pC/N and $k_p\sim44\%$ were acquired at $x=1.2$ when the ceramics were sintered at 1250 °C. The d_{33} value obtained is even higher than that for pure BZT sintered at 1400 °C (with $d_{33}\sim306$ pC/N), while the sintering temperature was lowered by 150 °C. The microstructure of the BZT ceramics was sensitive to the sintering temperature. With the increasing of sintering temperature, the grain morphology changed from spherical to elongated. Meanwhile, the abnormal grain growth (AGG) occurred at the higher sintering temperatures, which resulted in faceted and straight grain boundaries with hill-and-valley shapes. AGG made grains growth up rapidly and all the fine grains were replaced by coarse grains finally. However, the further increased sintering temperature led to the occurrence of amorphous intergranular phase, which may suppress the piezoelectric properties of ceramics. The excellent piezoelectric and electrical properties obtained in the low temperature sintered CuO-modified BZT ceramics render them good candidates for lead-free piezoelectric applications.

Acknowledgments

This work was supported by the National Natural Science Foundation of China (Grant no. 61071017), the Program for Cultivation of Academic & Technological Leaders in Sichuan Province, China (Grant no. 2012DTPY012) and the Program for Distinguished Young Scholar of Sichuan University (Grant no. 2011SCU04A05).

References

[1] W. Li, J.X. Zhi, Q.C. Rui, F. Peng, Z.Z. Guo, Enhanced ferroelectric properties in $(Ba_{1-x}Ca_x)(Ti_{0.94}Sn_{0.06})O_3$ lead-free ceramics, J. Eur. Ceram. Soc. 32 (2012) 517–520.

[2] W.F. Liu, X.B. Ren, Large piezoelectric effect in Pb-free ceramics, Phys. Rev. Lett. 103 (2009) 257602.
[3] J.G. Wu, D.Q. Xiao, W.J. Wu, J.G. Zhu, J. Wang, Effect of dwell time during sintering on piezoelectric properties of $(Ba_{0.85}Ca_{0.15})(Ti_{0.90}Zr_{0.10})O_3$ lead-free ceramics, J. Alloys Compd. 509 (2011) L359–L361.
[4] M. Tanmoy, R. Guo, A.S. Bhalla, Structure–property phase diagram of $BaZr_xTi_{1-x}O_3$ system, J. Am. Ceram. Soc. 91 (2008) 1769–1780.
[5] F. Mouraa, A.Z. Simoes, B.D. Stojanovic, M.A. Zaghete, E. Longoa, J.A. Varela, Dielectric and ferroelectric characteristics of barium zirconate titanate ceramics prepared from mixed oxide method, J. Alloys Compd. 462 (2008) 129–134.
[6] W. Li, Z.J. Xu, R.Q. Chu, P. Fu, G.Z. Zang, Dielectric and piezoelectric properties of $Ba(Zr_xTi_{1-x})O_3$ lead-free ceramics, Braz. J. Phys. 40 (2010) 353–356.
[7] N. Nanakorn, P. Jalupoom, N. Vaneesorn, A. Thanaboonsombut, Dielectric and ferroelectric properties of $Ba(Zr_xTi_{1-x})O_3$ ceramics, Ceram. Int. 34 (2008) 779–782.
[8] S.J. Kuang, X.G. Tang, L.Y. Li, Y.P. Jiang, Q.X. Liu, Influence of Zr dopant on the dielectric properties and Curie temperatures of Ba $(Zr_xTi_{1-x})O_3$ $(0 \leq \underline{x} \leq 0.12)$ ceramics, Scr. Mater. 61 (2009) 68–71.
[9] W.Q. Cao, J.W. Xiong, J.P. Sun, Dielectric behavior of Nb-doped Ba $(Zr_xTi_{1-x})O_3$, Mater. Chem. Phys. 106 (2007) 338–342.
[10] X.G. Tang, J. Wang, X.X. Wang, H.L.W. Chan, Effects of grain size on the dielectric properties and tunabilities of sol–gel derived $Ba(Zr_{0.2}Ti_{0.8})O_3$ ceramics, Solid State Commun. 131 (2004) 163–168.
[11] Y.L. Wang, L.T. Li, J.Q. Qi, Z.L. Gui, Ferroelectric characteristics of ytterbium-doped barium zirconium titanate ceramics, Ceram. Int. 28 (2002) 657–661.
[12] P. Zheng, J.L. Zhang, H.B. Qin, K.X. Song, J. Wu, Z.H. Ying, L. Zheng, J.X. Deng, MnO_2-modified $Ba(Ti,Zr)O_3$ ceramics with high Q_m and good thermal stability, J. Electron. Mater. 42 (2013) 1154–1157.
[13] X.J. Chou, J.W. Zhai, X. Yao, Relaxor behavior and dielectric properties of $MgTiO_3$-doped $BaZr_{0.35}Ti_{0.65}O_3$ composite ceramics for tunable applications, J. Am. Ceram. Soc. 90 (2007) 2799–2801.
[14] C. Ciomaga, M. Viviani, M.T. Buscaglia, V. Buscaglia, L. Mitoseriu, A. Stancu, P. Nanni, Preparation and characterisation of the $Ba(Zr,Ti)O_3$ ceramics with relaxor properties, J. Eur. Ceram. Soc. 27 (2007) 4061–4064.
[15] T. Maiti, E. Alberta, R. Guo, and A. S. Bhalla, The Polar Cluster like Behavior in Ti4+ Substituted BaZrO3 Ceramics, Matter. Lett. 60 (2006) 3861–3865.
[16] P. Zheng, J.L. Zhang, S.F. Shao, Y.Q. Tan, C.L. Wang, Piezoelectric properties and stabilities of CuO-modified $Ba(Ti,Zr)O_3$ ceramics, Appl. Phys. Lett. 94 (2009) 032902.
[17] D.M. Lin, K.W. Kwok, H.L.W. Chan, Piezoelectric and ferroelectric properties of $K_xNa_{1-x}NbO_3$ lead-free ceramics with MnO_2 and CuO doping, J. Alloys Compd. 461 (2008) 273–278.
[18] H.E. Mgbemere, R.-P. Herber, G.A. Schneider, Effect of MnO_2 on the dielectric and piezoelectric properties of alkaline niobate based lead free piezoelectric ceramics, J. Eur. Ceram. Soc. 29 (2009) 1729–1733.
[19] W.-G. Yang, B.-P. Zhang, N. Ma, L. Zhao, High piezoelectric properties of $BaTiO_3$–xLiF ceramics sintered at low temperatures, J. Eur. Ceram. Soc. 32 (2012) 899–904.
[20] P. Jarupoom, K. Pengpat, G. Rujijanagul, Enhanced piezoelectric properties and lowered sintering temperature of $Ba(Zr_{0.07}Ti_{0.93})O_3$ by B_2O_3 addition, Curr. Appl. Phys. 10 (2010) 557–560.
[21] C.-S. Chou, C.-L. Liu, C.-M. Hsiung, R.-Y. Yang, Preparation and characterization of the lead-free piezoelectric ceramic of $Bi_{0.5}Na_{0.5}TiO_3$ doped with CuO, Powder Technol. 210 (2011) 212–219.
[22] W. Jo, J.-B. Ollagnier, J.-L. Park, E.-M. Anton, O.-J. Kwon, C. Park, H.-H. Seo, J.-S. Lee, E. Erdemd, R.-A. Eichel, J. Rödel, CuO as a sintering additive for $(Bi_{1/2}Na_{1/2})TiO_3$–$BaTiO_3$–$(K_{0.5}Na_{0.5})NbO_3$ lead-free piezoceramics, J. Eur. Ceram. Soc. 31 (2011) 2107–2117.
[23] H.-Y. Park, J.-Y. Choi, M.-K. Choi, K.-H. Cho, S. Nahmw, Effect of CuO on the sintering temperature and piezoelectric properties of $(Na_{0.5}K_{0.5})NbO_3$ lead-free piezoelectric ceramics, J. Am. Ceram. Soc. 91 (2008) 2374–2377.
[24] F. Azough, M. Wegrzyn, R. Freer, S. Sharma, D. Hall, Microstructure and piezoelectric properties of CuO added $(K,Na,Li)NbO_3$ lead-free piezoelectric ceramics, J. Eur. Ceram. Soc. 31 (2011) 569–576.
[25] H.-Y. Park, C.-W. Ahn, K.-H. Cho, S. Nahmw, Low-temperature sintering and piezoelectric properties of CuO-added $0.95(Na_{0.5}K_{0.5})NbO_3$–$0.05BaTiO_3$ ceramics, J. Am. Ceram. Soc. 90 (2007) 4066–4069.
[26] N. Binhayeeniyi, P. Sukvisut, C. Thanachayanont, S. Muensit, Physical and electromechanical properties of barium zirconium titanate synthesized at low-sintering temperature, Mater. Lett. 64 (2010) 305–308.
[27] P. Zheng, K.X. Song, H.B. Qin, L. Zheng, L.M. Zheng, Piezoelectric activities and domain patterns of orthorhombic $Ba(Zr,Ti)O_3$ ceramics, Curr. Appl. Phys. 13 (2013) 1064–1068.
[28] T. Chen, T. Zhang, G.C. Wang, J.F. Zhou, J.W. Zhang, Y.H. Liu, Effect of CuO on the microstructure and electrical properties of $Ba_{0.85}Ca_{0.15}$-$Ti_{0.90}Zr_{0.10}O_3$ piezoceramics, J. Mater. Sci. 47 (2012) 4612–4619.
[29] C.W. Park, D.Y. Yoon, Effects of SiO_2, CaO_2, and MgO additions on the grain growth of alumina, J. Am. Ceram. Soc. 83 (2000) 2605–2609.
[30] Y.K. Cho, S.-J. Kang, D.Y. Yoon, Dependence of grain growth and grain-boundary structure on the Ba/Ti ratio in $BaTiO_3$, J. Am. Ceram. Soc. 87 (2004) 119–124.
[31] Y.-S. Yoo, H. Kim, D.-Y. Kim, Effect of SiO_2 and TiO_2 addition on the exaggerated grain growth of $BaTiO_3$, J. Eur. Ceram. Soc. 17 (1997) 805–811.
[32] W. Jo, D.-Y. Kim, N.-M. Hwang, Effect of interface structure on the microstructural evolution of ceramics, J. Am. Ceram. Soc. 89 (2006) 2369–2380.